# CHAPTER 4

# RESULTS AND DISCUSSIONS

## 4.1 Introduction

In this chapter, the data obtained – following the methods explained and analyzed in Chapter 3 will be presented and discussed. This chapter explains the results from the samples achieved and characterizations of the PHB/UDMA polymer blend.

## 4.2 Viscosity of PHB/UDMA Resin Blend

Viscosity is an indicator measurement of a fluid's resistance to flow. Pure UDMA resin has a viscosity of 1120 cP at room temperature. Gradually, the viscosity of the PHB/UDMA resin blend increases as PHB incorporated within the polymer matrix (resin) increases. 13 wt. % of PHB/UDMA resin blend could not be printed due to higher concentration of PHB powder. The printability of the resin blend is observed to reach optimal PHB content at 11 wt. % of PHB/UDMA with viscosity of 2188 cP. The red line indicate the highest viscosity could reach to define a success printability of 3D structures. Figure 4.1 depicts the graph of pure UDMA resin and different weight percentage of PHB content within UDMA resin.

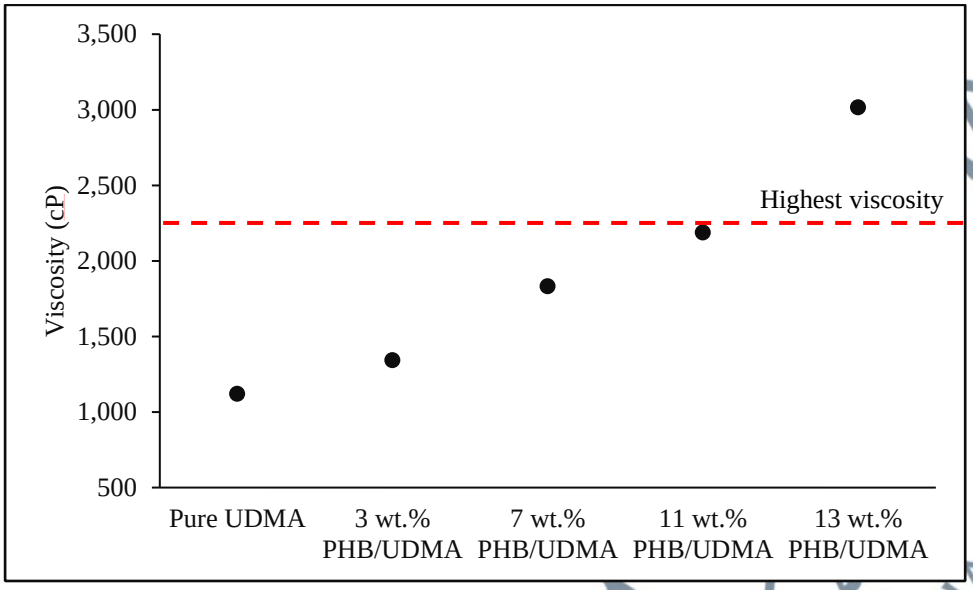


**Figure 4.1:** The Viscosity of Pure UDMA Resin and PHB/UDMA Resin Blend.

## 4.3 Tensile Properties

According to the Shapiro-Wilk test, the data of tensile properties are normally distributed since all the compositions of 3D printed PHB/UDMA showed a significant value of $P > 0.05$. Therefore, two-way analysis of variance (ANOVA) has selected as a statistical test to study the significant effect of PHB content (wt. %) incorporated within UDMA based resin and the aging duration of 3D printed PHB/UDMA towards tensile properties, which denotes as A and B respectively. The dependent variables comprise of Young's modulus, tensile stress and tensile strain are assessed separately. There are two hypotheses generated, called null hypothesis and alternative hypothesis, $H_0$ and $H_1$ respectively. $H_0$ stated that there is no interaction found, whilst $H_1$ stated that there is interaction found, between those factors towards tensile properties. The hypothesis would be decided according to F-value. Meanwhile, P-value is utilized to decide the validity of null hypothesis.

For instance, the significance study of the weight percentage (wt. %) of PHB induced within UDMA resin towards Young's modulus is evaluated by using F-Table.

The critical value shown in F-Table (=4.07) is smaller than F-value (=7.34) depicted in Table 4.1 at significance of α=0.05. Therefore, in this case, null hypothesis is rejected. To verify the validity of the null hypothesis being rejected, P-value is calculated using F-value. P-value is obtained at P=0.003, which was P<0.05. In conclusion, there is a statistically significant interaction between the weight percentage (wt. %) of PHB induced within UDMA resin towards Young's modulus. The F and P-value of these two independent variables towards tensile characteristics (Young's modulus, tensile stress, and tensile strain) are established after using the same approach to the period of aging duration as well as the interaction between both of them. Results in Table 4.1 also shows that Young's modulus, tensile stress and tensile strain are highly significant influenced by the weight percentage (wt. %) of PHB inclusion into UDMA resin, the period of aging duration and the interaction between both of them.

**Table 4.1:** Statistical Analysis using Two-Way ANOVA for Tensile Properties.

| **Two-Way** | **Young's modulus** | | | **Tensile stress** | | | **Tensile strain** | | |
|---|---|---|---|---|---|---|---|---|---|
| **ANOVA** | **A** | **B** | **A × B** | **A** | **B** | **A × B** | **A** | **B** | **A × B** |
| DF | 3 | 1 | 3 | 1 | 3 | 1 | 3 | 1 | 3 |
| S | 0.183 | 193.04 | 0.089 | 699.88 | 129.18 | 65.74 | 32.74 | 678.83 | 17.50 |
| S | 0.061 | 193.04 | 0.030 | 233.29 | 129.18 | 21.91 | 10.91 | 678.83 | 5.84 |
| F-value | 7.34 | 23,277.33 | 3.57 | 44.16 | 24.45 | 4.15 | 15.02 | 934.19 | 8.03 |
| P-value | 0.003 | 0.000 | 0.038 | 0.000 | 0.000 | 0.024 | 0.000 | 0.000 | 0.002 |

DF = Degree of freedom
SS = Sum of squares
MS = Mean square
A = Effect of the PHB content (wt. %) within UDMA based resin towards tensile properties
B = Effect of aging duration towards tensile properties
A × B = Effect of the interaction between A and B towards tensile properties

A gradual decrease in the tensile stress is observed with the increase in the percentage of PHB powder. Three significant factors that affected the tensile strength in particle-polymer composites are size of the particle, percentage content of particle and the interfacial adhesion of particle/matrix. Poor interfacial adhesion between the PHB powder and UDMA resin contributes towards the declination of tensile strength.

Moreover, PHB powder tend to agglomerate at higher concentration of PHB forming a local region of stress. The irregular distribution of PHB agglomeration causes the transfer of stress to become non-uniform. Hence, the formation of cracks is created around the stressed region. The interpretation of the agglomeration phenomenon is presented by FESEM in Section 4.7.

Tensile strain is the percentage change of length from its initial dimension to failure. In simpler words, the ability of materials to deform or bending without breaking. Tensile strain decrease steadily along the increment of PHB powder incorporation. The highest is recorded at 2.30% for pure UDMA, whilst 11 wt. % of PHB/UDMA has a reduction of elongation at break about 35% after a day of aging. Similar pattern could be observed after a month of aging. Therefore, the inclusion of PHB particles that acting as filler has restricted the mobility of the molecular chain of UDMA deformation.

Young's modulus is defined as capability of an object to deform along an axis of the applied forces. In layman terms, it is an indicator for stiffness of a certain object or material. Young's modulus portrayed a slight increment along the inclusion of PHB powder. 11 wt. % of PHB/UDMA obtained a highest value at 6.60 GPa whilst pure UDMA was measured at 6.28 GPa. PHB is categorized as semi-crystalline polymer whilst UDMA as an amorphous solid polymer. Hence, the inclusion of rigid particles can increase the modulus since the rigidity of PHB powder (filler) much higher than the UDMA (matrix). Table 4.2 and Table 4.3 show the measurements of tensile properties after a day and a month of aging respectively.

**Table 4.2:** Tensile Properties of 3D Printed PHB/UDMA over a Day.

| Composition name | Tensile strength (MPa) | Elongation at break (%) | Young's modulus (GPa) |
|---|---|---|---|
| 0 wt. % PHB/UDMA | 83.65 ± 2.57 | 2.30 ± 1.64 | 6.28 ± 0.12 |
| 3 wt. % PHB/UDMA | 80.20 ± 0.96 | 2.13 ± 0.07 | 6.25 ± 0.05 |
| 7 wt. % PHB/UDMA | 71.78 ± 1.55 | 1.78 ± 0.12 | 6.47 ± 0.18 |
| 11 wt. % PHB/UDMA | 67.70 ± 1.58 | 1.44 ± 0.07 | 6.60 ± 0.12 |

**Table 4.3:** Tensile Properties of 3D Printed PHB/UDMA over a Month.

| Composition name | Tensile strength (MPa) | Elongation at break (%) | Young's modulus (GPa) |
|---|---|---|---|
| 0 wt. % PHB/UDMA | 73.28 ± 2.75 | 14.20 ± 1.20 | 0.65 ± 0.03 |
| 3 wt. % PHB/UDMA | 77.72 ± 2.75 | 14.82 ± 1.20 | 0.74 ± 0.03 |
| 7 wt. % PHB/UDMA | 68.90 ± 2.73 | 11.20 ± 1.20 | 0.76 ± 0.03 |
| 11 wt. % PHB/UDMA | 64.85 ± 2.70 | 9.98 ± 1.20 | 0.76 ± 0.03 |

## 4.4 Impact

The data of impact strength portrays a normal distribution concordance to Shapiro-Wilk test. Two-way ANOVA is executed to analyze the significant effect of weight percentage (wt. %) of PHB inclusion within UDMA, aging duration of 3D printed PHB/UDMA and both of them towards impact strength. Null and alternative hypotheses are also established accordingly with the same approach as aforementioned in tensile section. The F-value (=9.134) shown in Table 4.4 is larger than critical F-value in F-Table (=4.07 at significance of $\alpha$=0.05. The null hypothesis is rejected where $P<0.05$. Therefore, the PHB content (wt. %) incorporated within UDMA resin has a statistically significant effect towards impact strength. However, during the period of aging, it is found to not have any statistically significant effect towards impact strength. This is might probably due to the time taken for a month is a short time.

**Table 4.4:** Statistical Analysis using Two-Way ANOVA for Impact Strength.

| Two-Way ANOVA | Impact strength | | |
|---|---|---|---|
| | A | B | A × B |
| DF | 3 | 1 | 3 |
| SS | 6.400 | 0.435 | 0.441 |
| MS | 2.133 | 0.435 | 0.147 |
| F-value | 9.134 | 1.861 | 0.630 |
| P-value | 0.001 | 0.191 | 0.606 |

DF = Degree of freedom
SS = Sum of squares
MS = Mean of square
A = Effect of the PHB content (wt. %) within UDMA based resin towards impact strength
B = Effect of aging duration towards impact strength
A × B = Effect of the interaction between A and B towards impact strength

The fracture toughness greatly influenced by particle size, interfacial adhesion of the two constituent materials and particle loading. Figure 4.2 presents the impact strength for pure UDMA which is measured at 4.91 kJ/m$^2$ whilst at 11 wt. % of PHB/UDMA, it is only obtained 3.33 kJ/m$^2$. At higher loading of PHB powder within the UDMA, the impact strength decreases gradually due to poor interfacial adhesion between both constituent materials. In particle-polymer composites, the particle and matrix has notable effect towards fracture toughness. Stronger adhesion typically contributes towards higher fracture of toughness for thermoplastic matrices.

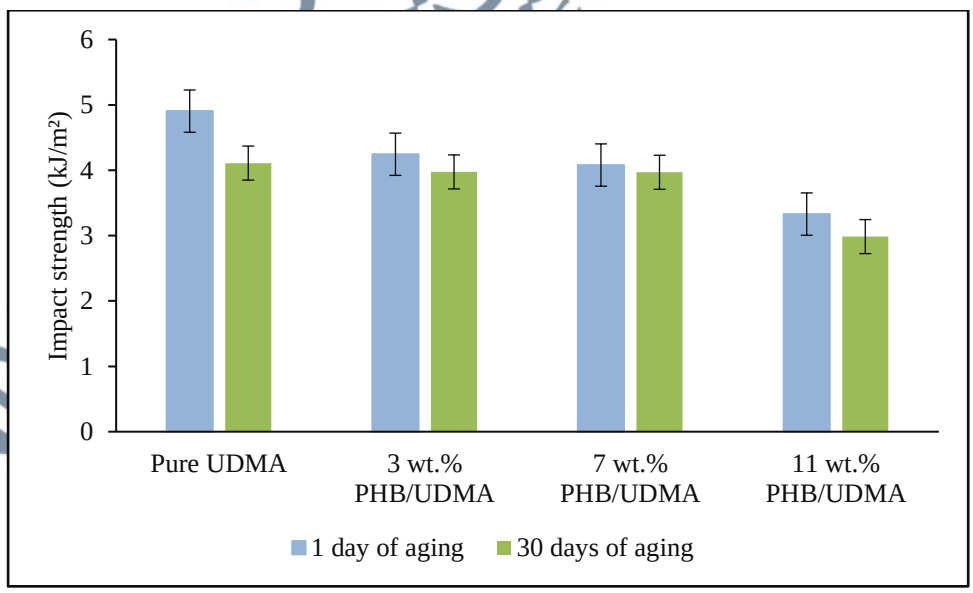


**Figure 4.2:** Impact Strength of 3D Printed PHB/UDMA.

The agglomeration of PHB particles which were acting as filler within the UDMA matrix caused the reduction in impact strength as the PHB contents increased. In composites, the agglomeration is a region that could act as a foreign body. When there were increments of agglomerates at higher PHB loading, PHB became obstacles that restricted the mobility of the UDMA molecular chain which later induced failure under stress. An increase in filler loading does not eventually strengthen the composites. In a certain case, it could weaken the materials, since more defects were created as the filler fractions become higher. Moreover, it is important to elucidate that brittleness of the composites was attributed to the resistance of PHB agglomerations against UDMA deformation. As a result, the propagation of cracks became much faster due to the lack of plastic deformation and failure to absorb energy. Thus, the impact strength of the particulate composite is highly affected by the filler volume fraction. In addition, the impact strength of the composite is also mainly attributed to its particle size, adhesion to the matrix, and the uniformity of their distribution in the polymer composite (Abu Bakar et al., 2022).

### 4.5 Fourier Transform Infrared (FTIR)

The absorbance peaks for PHB powder are consistent with those discovered in previous studies (Trakunjae et al., 2021). The C=O stretching modes in the molecular chain correlate to the ester carbonyl group peak, which is situated at 1729 $cm^{-1}$. 1279 $cm^{-1}$ corresponds to the adsorption band at the C-H group (ester bonding). C-O stretching modes portrayed a series of bands ranging from 1163 $cm^{-1}$ to 1210 $cm^{-1}$. Functional group of methyl are observed to appear at 2969 and 2927 $cm^{-1}$, with its symmetric bending at 1377 $cm^{-1}$. The biaxial bending of $–CH_3$ and $–CH_2$ is depicted at

1452 $cm^{-1}$ and lastly an indistinct peak appeared at 3434 $cm^{-1}$ is belonged to the hydroxyl group. Figure 4.3 presents the absorbance peaks of FTIR for PHB powder.

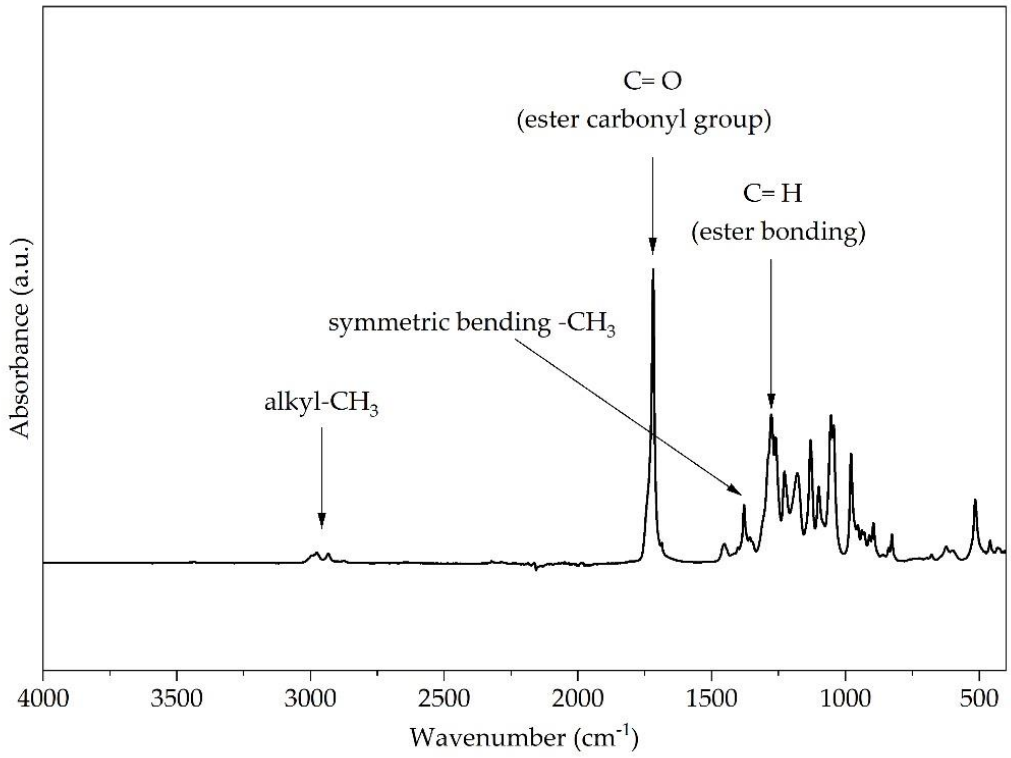


**Figure 4.3:** The Absorbance Peaks of Infrared (IR) Spectrum for PHB.

1,6-bis(metalocriloxi-2-etoxicarbolamino)-2,4,4-trimethylexane is the chemical name for UDMA. It has two urethane linkages and an aliphatic core. The C=O stretching mode is shown by a distinct absorbance peak at 1709 $cm^{-1}$, whereas the C=C stretching mode appeared at 1637 $cm^{-1}$. The stretching modes of urethane functional groups are depicted by a broader peak ranging from 3200 until 3400 $cm^{-1}$ whilst its bending is located at 1634 $cm^{-1}$. Finally, the vibrational motion of C−H stretching appeared at a range of wavenumbers approximately within 2800 and 3000 $cm^{-1}$. Figure 4.4 shows a series of IR spectra for UDMA resin, 3D printed UDMA and 3D printed PHB/UDMA.

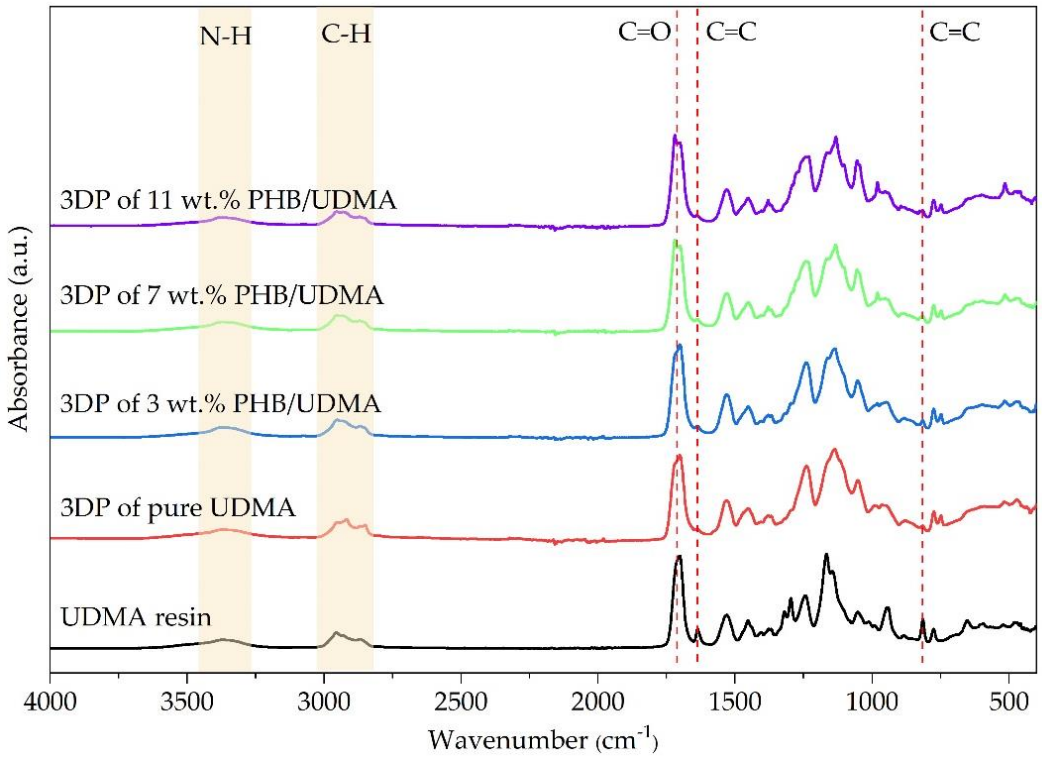


**Figure 4.4:** The Absorbance Graphs of Infrared (IR) Spectra for UDMA Resin, 3D Printed UDMA and 3D Printed PHB/UDMA.

The degree of double bond conversion (DC) is typically utilized to further clarify the structure and properties of the dimethacrylate polymer network. The vinyl group's stretching mode and the carbon-carbon double bond's twisting mode, respectively, are represented by the peaks at 1637 $cm^{-1}$ and 816 $cm^{-1}$, respectively. Those two peaks are commonly used to evaluate the polymerization of acrylates and methacrylates polymer. However, the peak located at 1637 $cm^{-1}$ is selected, attributed from its distinct appearance instead of the other one. The intensity of the peaks acts as an indicator of the vinyl double bonds that remained after the polymerization took place.

During the polymerization in poly(dimethacrylate), the conversion of monomer never complete and the residual of the unreacted double bonds will remain as methacrylate pendant groups. The degree of conversion of monomer to polymer in resin

composites is typically ranging between 35% and 77%. The formation of gel sol fraction that prevents the complete polymerization from happened and thus blocks the polymeric network. The leaching of unreacted monomers can cause inflammation towards human health. Therefore, a standard of DC has been set for the clinical application whereas the DC must be at least 55% for the therapeutic usage (Barszczewska-Rybarek, 2019). In general, incomplete polymerization of photopolymer resin can induce the leaching of unreacted monomer. The DC for 3D printed UDMA was evaluated at 63.73%. The DC for 7 wt. % and 11 wt. % of PHB/UDMA have passed minimum level and achieved at 55.68 % and 56.86 % respectively. Figure 4.5 presents the bar chart of DC for 3D printed UDMA and PHB/UDMA.

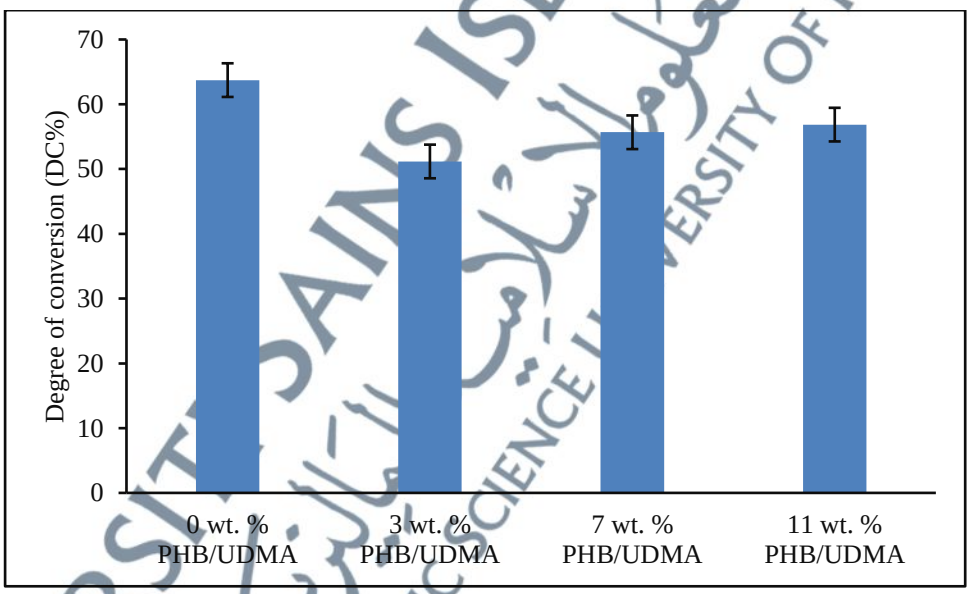


**Figure 4.5:** Degree of Double Bonds Conversion for 3D Printed PHB/UDMA.

## 4.6 X-Ray Diffraction (XRD)

Information about the parameters including peaks and full width at height maxima (FWHM) are presented in Table 4.5. All of these information are the result of the deconvolution process and curve-fitting of several crystalline peaks of PHB powder.

The average of crystallite size of PHB powder is measured by using Scherrer formula and obtained at 15.33 nm as shown in Table 4.5.

**Table 4.5:** The Average of Crystallite Size of PHB Powder.

| Peak Position, 2θ (°) | FWHM, β (Radian) | Crystallite size, D (nm) | Average crystallite size, D (nm) |
|---|---|---|---|
| 13.44 | 0.32085 | 24.7605 | |
| 16.85 | 0.39556 | 20.0841 | |
| 20.01 | 14.3158 | 0.5727 | |
| 21.65 | 1.67154 | 4.7547 | 15.33 |
| 22.61 | 0.64941 | 12.2339 | |
| 25.45 | 0.61602 | 12.8969 | |
| 27.10 | 0.24812 | 32.0182 | |

PHB exhibits several crystalline peaks at 2θ = 13.5°, 16.9°, 21.5° and 22.6°. Two sharp peaks with strong intensity are detected at 2θ = 13.5° and 16.9°, and are assigned to be (020) and (110) respectively, attributed from its orthorhombic unit cell respectively. The reflections angle of scattering at two latter angles belongs to α PHB crystal structure concordance with the (101) and (111). Contrary with the amorphous solid materials, they do not have a definite lattice pattern. Therefore, 3D printed UDMA only shows a broader hump of XRD pattern due to its amorphous characteristic. Figure 4.6 shows the XRD profile for PHB powder, 3D printed pure UDMA and PHB/UDMA.

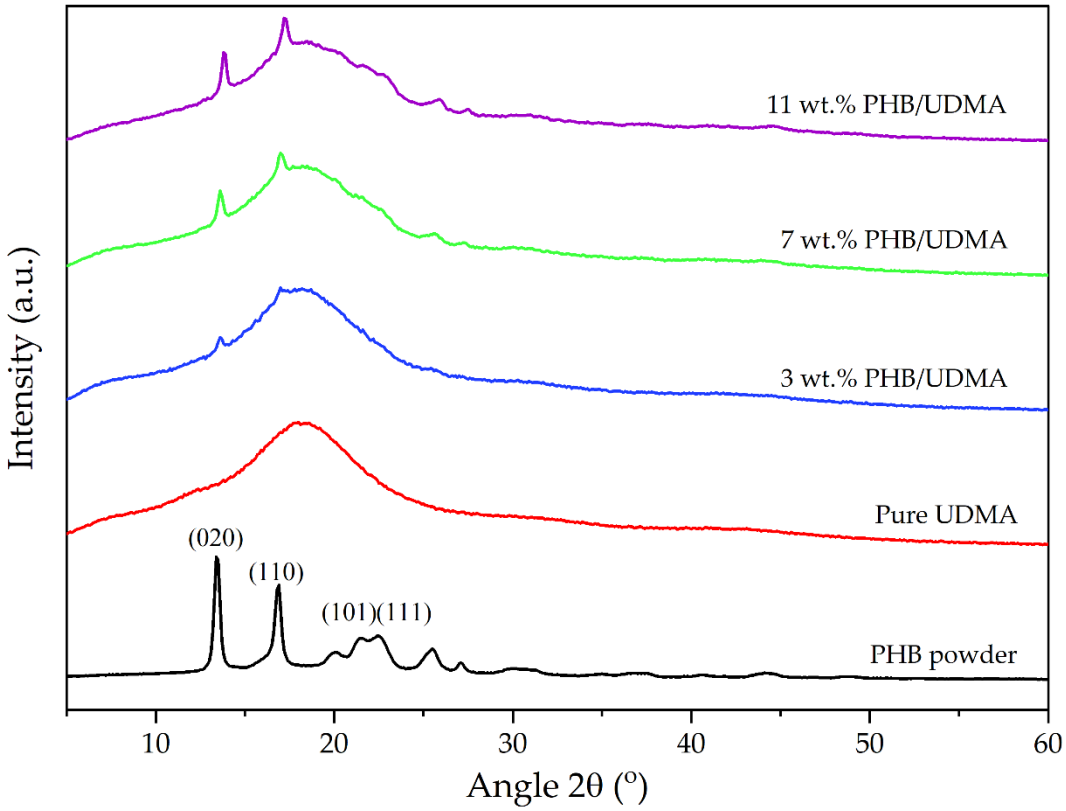


**Figure 4.6:** The XRD Profile of PHB Powder and 3D Printed PHB/UDMA.

A parameter known as crystallinity index (CI) is a quantitative indicator of crystallinity. PHB powder is obtained at 91.52% of CI. The higher weight percentage (wt. %) of PHB powder inclusion within UDMA, the more apparent the crystalline peaks belongs to the PHB starts to appear in the 3D printed PHB/UDMA. 11 wt. % of PHB/UDMA shows the highest CI at a value of 34.98%. Figure 4.7 shows bar chart of crystallinity index (CI) for PHB powder, 3D printed UDMA and PHB/UDMA.

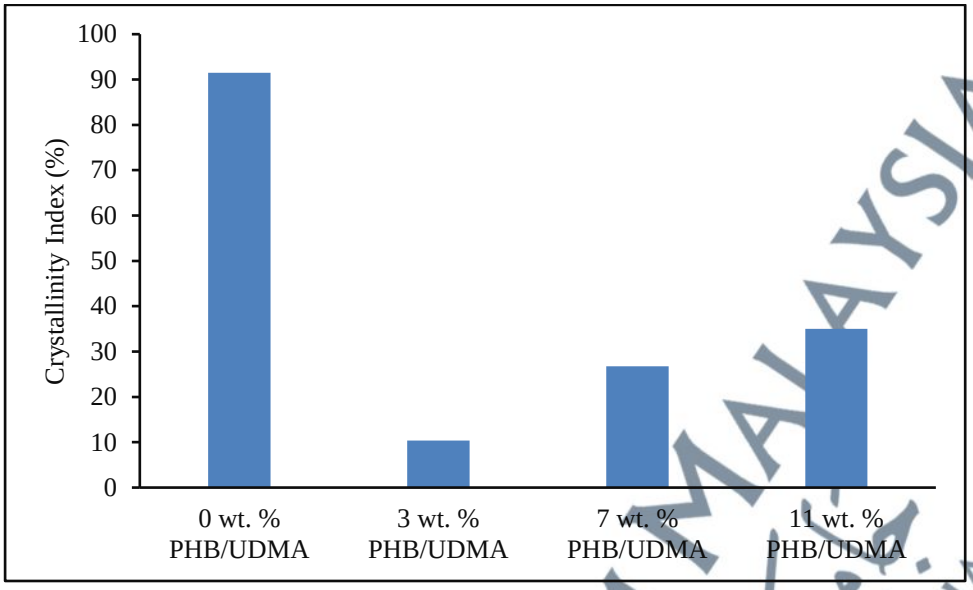


**Figure 4.7:** Crystallinity Index of 3D Printed PHB/UDMA.

## 4.7 Field-Emission Scanning Electron Microscope (FESEM)

FESEM images are obtained to evaluate the surface morphology of 3D printed PHB/UDMA. Pure UDMA displays a smooth lamellar structure of typical amorphous solid polymer. Non-uniform spherical particles of surface for PHB/UDMA indicates the ubiquitous of PHB powder. As the weight percentage (wt. %) of PHB increases, the agglomeration of PHB became more apparent and the cavities/voids also started to emerge. The dispersed phase could be observed that indicates poor interfacial adhesion between two phases; PHB (particle) and UDMA (matrix).

Since PHB and UDMA are not compatible to each other, they are classified as a heterogeneous mixture. Therefore, in two phased materials, one component typically undergoes deformation less than the others. The plastic deformation is greatly influenced by the microstructure in the particulate-matrix composites. As the PHB agglomerates in cluster, its diameter increases in the second phase. Thus, the effects of the aggregation of particles as cluster can be correlated with the decrease of the tensile and impact strength. Hence, the reduction of mechanical performance is in accordance

with the surface morphology of 3D printed PHB/UDMA. Figure 4.8 shows the FESEM images of surface morphology for 3D printed UDMA and PHB/UDMA.

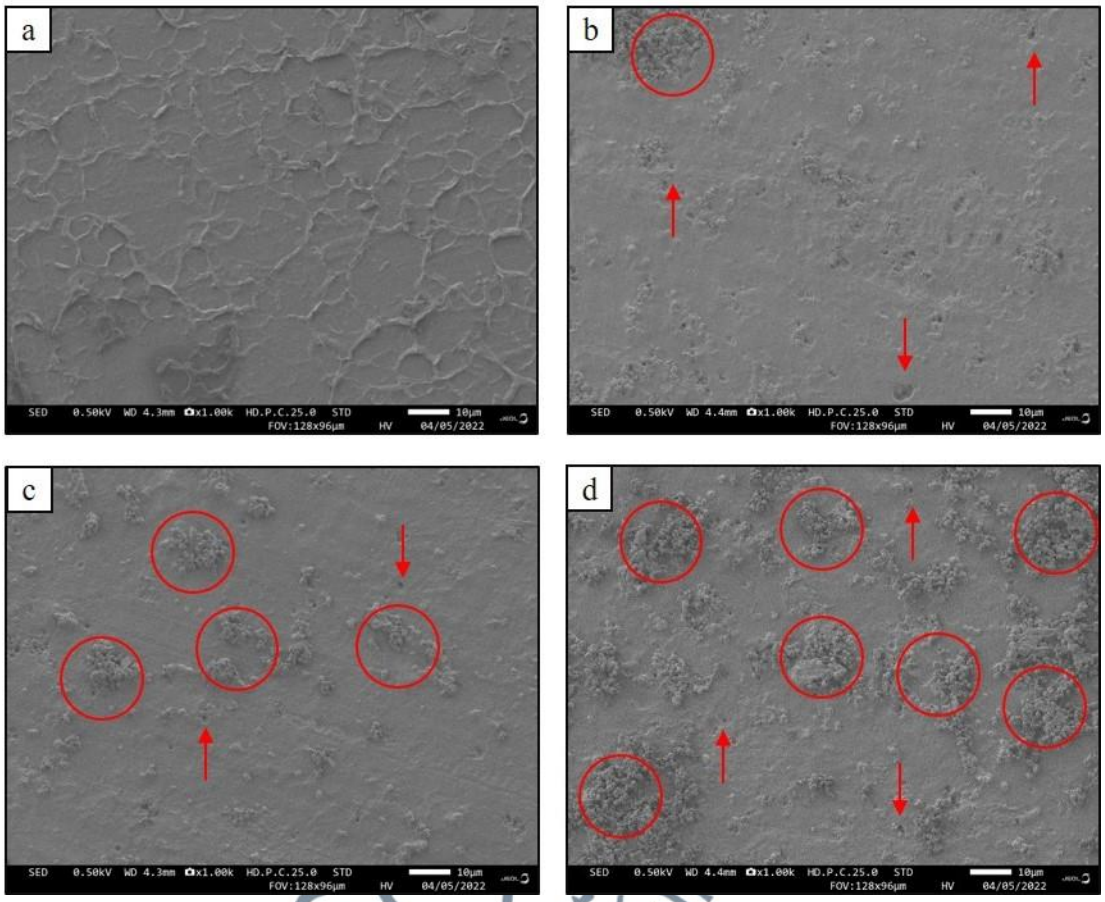


**Figure 4.8**: Surface Morphology of 3D Printed: a) UDMA; b) 3 wt. % PHB/UDMA; c) 7 wt. % PHB/UDMA and d) 11 wt. % PHB/UDMA.

## 4.8 Thermogravimetric Analysis (TGA)

It is apparent that PHB powder only exhibits a single step degradation from 262 °C until 326 °C. A prominent peak is observed at 305 °C for the maximum rate of degradation, leaving a residue of 4.94% as shown in Figure 4.9. β-elimination is the basic pyrolysis mechanism of PHB that facilitates the formation of crotonic acid, dimeric, trimeric and tetrameric volatiles.

Meanwhile, photopolymer resin is anticipated to have two or three steps degradation mechanism. It is correlated with the experimental findings that the ubiquitous of two steps degradation for 3D printed UDMA. It is started at 262 °C and ended at 496 °C, leaving out only 6.65% of solid residue. The annihilation of dismutation reaction during the polymerization contributes to the random scission of vinylidene end groups for the first step of degradation, whilst the latter one is induced by the random scission of abnormal head-to-head linkages. The thermogravimetric analysis (TGA) and derivative of TGA (dTGA) curves are shown in Figure 4.10 and Figure 4.11 respectively.

There are three steps of thermal degradation for 3D printed PHB/UDMA. An extra peak will start to form as the PHB content are increased. The initial peak for the rate of thermal degradation curve began to move to the lower temperature. As indicated in Table 4.6, they are appeared at 341 °C, 335 °C, 327 °C for 3, 7 and 11 wt. % PHB/UDMA, respectively.

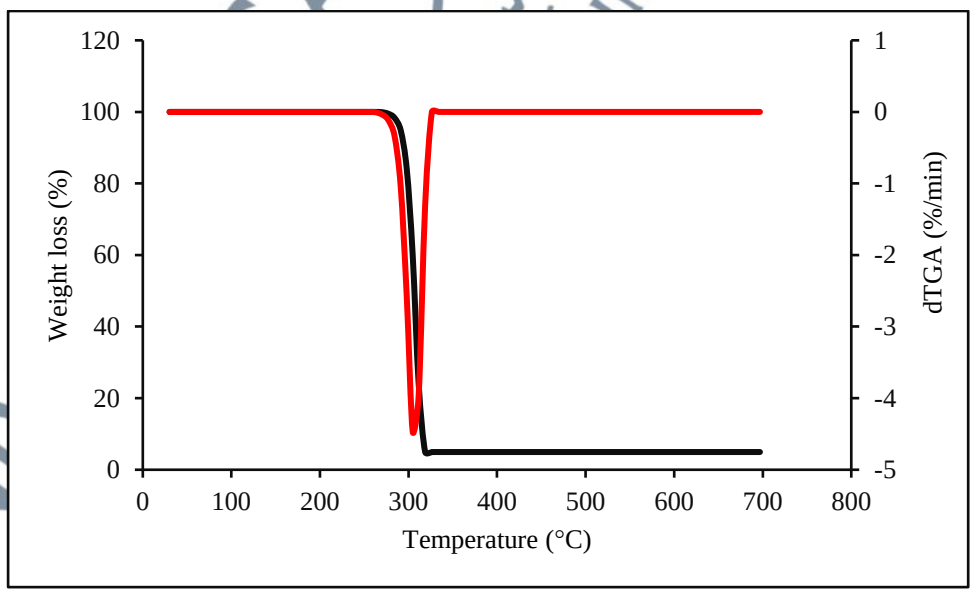


**Figure 4.9:** TGA and DTGA of PHB Powder.

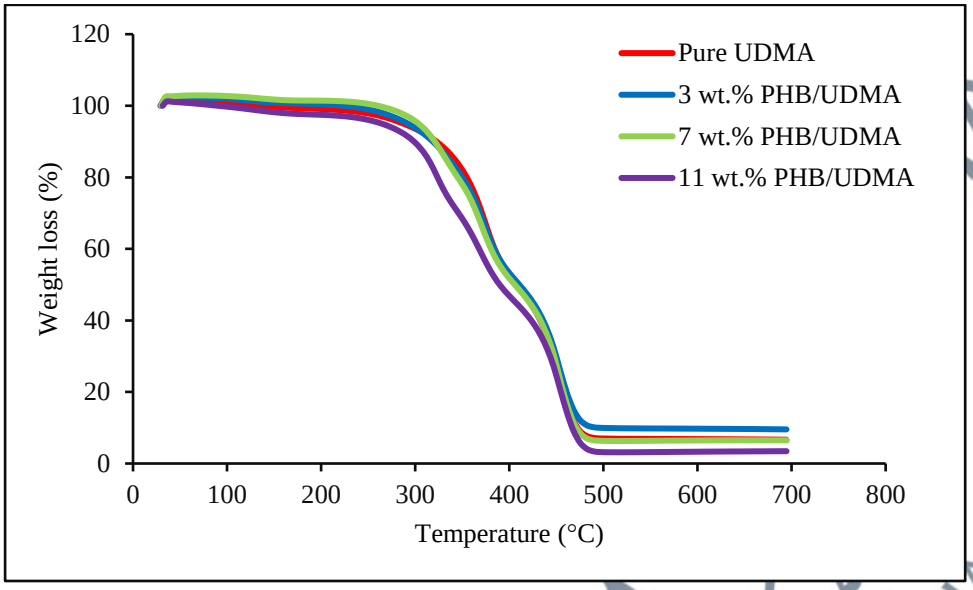


**Figure 4.10:** TGA of 3D Printed PHB/UDMA.

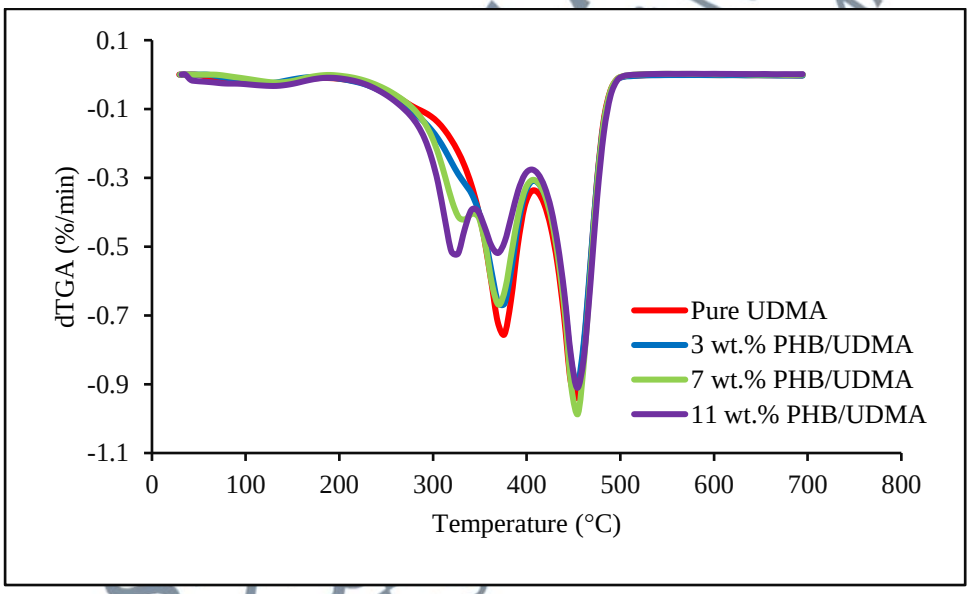


**Figure 4.11:** DTGA of 3D Printed PHB/UDMA.

**Table 4.6:** The Parameters Extracted from TGA and DTGA Curves.

| Sample | PHB | UDMA | 3 wt. % of PHB/UDMA | 7 wt. % of PHB/UDMA | 11 wt. % of PHB/UDMA |
|---|---|---|---|---|---|
| $T_1$ (°C) | 262-326 | 262-411 | 298-348 | 263-342 | 262-341 |
| $T_2$ (°C) | - | 411-496 | 348-405 | 342-406 | 341-405 |
| $T_3$ (°C) | - | - | 405-510 | 406-504 | 405-510 |
| Residual weight (%) | 4.95 | 6.65 | 9.53 | 6.47 | 3.45 |

## 4.9 3D Printed Arm Cast

The concept of additive manufacturing for 3D printed arm cast revolve around its several features such as lightweight, appropriate fit and ventilated structure. It should be noted that the subject used for this study is only a normal man with ideal body mass index to act as a fracture-bone arm patient. The process is started with the 3D scanning procedure to obtain images data of his arm with 3D spatial information. The arm is positioned and maintained at a relative support during the scanning phase for several minutes. The 3D mesh images are then transferred into a computer for further reconstruction in computer-aided design (CAD) software. The ventilation structure of 3D mesh is also generated as an inspiration of additive manufacturing for diminishing the risk of irritation and the convenience of a regular inspection as well as reducing the overall device weight.

As soon as the scanning and designation of the arm are completed, the 3D images are sliced through a slicer software (Cura) to convert the 3D images file into standard triangulated language (STL) file that is readable for the stereolithography (SLA) 3D printer. 7 wt. % of PHB/UDMA formulation is selected to develop the 3D printed arm cast based on the preceding analysis. The normal exposure time of the laser towards the PHB/UDMA resin blends is set at 60 s. After the printing process is finished, the cast is cleaned and washed by isopropanol to remove all the uncured resin. Finally, the cast is further cured by the ultraviolet (UV) light for about an hour. Figure 4.12 displays an overview for the development of 3D printed arm cast, whilst Figure 4.13 shows the 3D model in STL file and actual 3D printed arm cast.

The requirement for the degree of double bond conversion had passed the minimum standard that has been set for clinical application. Since the rehabilitation process typically takes about four to six weeks, the mechanical performance must be

able to maintain within the period. Hence, the inclusion of PHB as additives in the UDMA resin had proven to retain its mechanical performance instead of utilizing UDMA alone. The declination of tensile strength for UDMA is approximately at 13% after a month of aging. However, the inclusion of PHB retains strength below than 3% of its reduction.

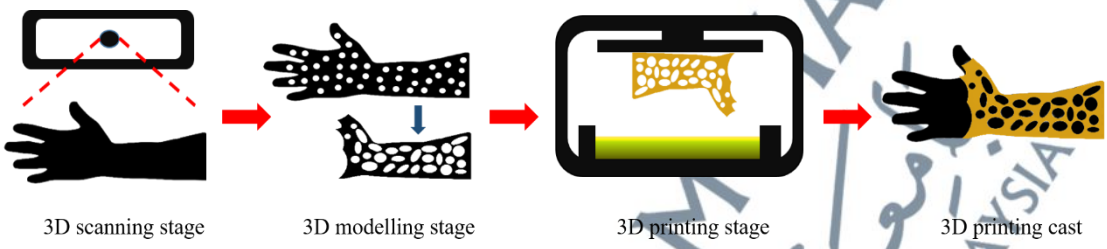


**Figure 4.12:** The Overview Process of 3D Printed Arm Cast.

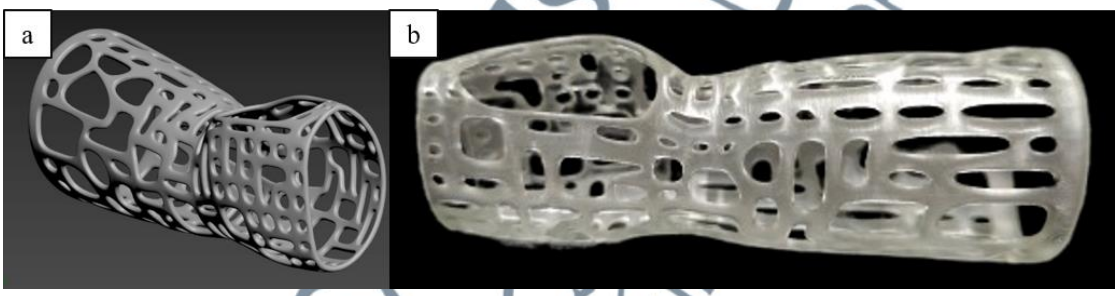


**Figure 4.13:** a) 3D Model Design; b) 3D Printed Arm Cast.